Characterization of Loading Environment on Human Ribs during Ventilation

Undergraduate Honors Thesis

Presented in Partial Fulfillment of the Requirements for

Graduation with Distinction

at The Ohio State University

By

Katherine M. Stemmer

The Ohio State University

2016

Defense Committee:

Professor John Bolte, Adviser

Assistant Professor Amanda Agnew

Research Scientist Yun-Seok Kang

Approved by

Adviser

Undergraduate Program in Biomedical Engineering

Abstract

The human thoracic cavity holds vital organs, such as the heart and lungs. The rib cage provides protection to these organs, and as a result is susceptible to injuries. One important determinant in the susceptibility of ribs, and bone in general, to fracture is the accumulation of microfractures. These microfractures occur in ribs due to cyclic loading and stress during normal ventilation. Since microfractures accumulate in regions of bone that experience high local strains, it is important to measure the strain patterns ribs experience during the regular loading environment of breathing. The strain mode of the cutaneous cortex and pleural cortex of the rib is unknown and failing to account for how the rib responds to the loading (i.e., initiates microfractures) will affect the accuracy of a physiological model. The objective of this study was to determine the strain modes and magnitudes experienced by the ribs during ventilation. One Post-Mortem Human Surrogate (PMHS) was instrumented with strain gages on the pleural and cutaneous surfaces of ribs 3-9, along with two strain gages on the sternum, resulting in a total of 86 gages. A bladder and air pump were used to mimic ventilation in a defined combination of shallow and deep breaths. Results include location comparisons in strain between bilateral rib pairs, quantification of variation in strain mode (tension versus compression) based on location, and differences in strain magnitudes along the length of the rib. These results will improve researchers' understanding of physiological strain in the ribs during

ventilation and potential for microfracture initiation and repair. A greater comprehension of fracture susceptibility will help researchers improve biofidelic models and their understanding of the loading environment to which the rib is adapted.

Acknowledgements

I would like to thank Dr. John Bolte, my advisor, for providing me with this wonderful opportunity to conduct biomedical engineering research and for continuously supporting me throughout the project. I would especially like to thank Dr. Amanda Agnew and Dr. Yun Seok Kang for their advice and support throughout the project. I would also like to thank Doctoral Student Ben Shurtz and Master student, Michelle Murach for their overall support of the project, as well as their help with comprehensive test preparation, experimentation, and data analysis. Additionally, I would like to thank the Injury Biomechanics Research Center (IBRC) at The Ohio State University for their financial support and the use of their facility's equipment. In particular, I would like to thank the employees of the IBRC, including Julie Bing and Allison Yard for their assistance during experimental setup, testing, and their continual support of the project.

Vita

NAME OF AUTHOR……..…Katherine Marie Stemmer

DATE AND PLACE OF BIRTH…… September 28, 1993, Dayton, OH

FIELDS OF STUDY…….. Biomedical Engineering

PUBLICATIONS:

Bodenstedt, S., Wagner, M., Mayer, B., Stemmer, K., Kenngott, H., Muller-Stich, B., . . . Speidel, S. (2016). Image-based laparoscopic bowel measurement. International Journal of Computer Assisted Radiology and Surgery, 11(3), 407-419.

Table of Contents

Table of Figures

List of Tables

Introduction

The human thorax plays an important role in protecting several organs including the heart, lungs, esophagus, and thymus. The ribs are an essential component of this protection and as such, many researchers conduct studies on them [1, 2]. However, one aspect of the ribs that is in need of further research is their potential to develop microfractures. Microfractures are cracks with a diameter around 500 μm that appear in bone as a result of physical activities [3]. This research aims to determine the effects of ventilation on the production of microfractures. The continual cycle of breathing instills a slight strain on the ribs and because microfractures are a common occurrence, it is important to determine their influence on rib strength and flexibility [4]. The compounding effects of microfractures could influence the ribs on a macroscale and potentially compromise the accuracy of rib models [5]. Therefore, the loading environment that ribs must adapt to during breathing needs to be studied in greater depth.

Ventilation is a remarkably dynamic process in the body. In the process of normal inspiration, a pressure change occurs and the external intercostal muscles assist by forcing the rib cage and sternum to rise. Studies have analyzed the deformation that the rib cage undergoes during inspiration, but individual rib distortion needs further investigation [6]. During voluntary, deep breathing, the muscles perform a more active role in expanding the rib cage to increase the pressure difference. This additional

voluntary movement causes greater distortion of the rib cage [6]. It is possible that the loading environment causes the rib to experience different polarity on different cortexes. The strain mode on ribs is an aspect of research that is not well studied but it could provide key information on how the rib would bend under different loading conditions.

Description of Ventilation and Thorax

This study is largely based on the movement of the thorax during ventilation, and it is therefore important to have an understanding of the process of ventilation and the anatomy of the thorax. Ventilation is the combination of inspiration and exhalation. For inspiration to occur during normal breathing, the pressure in the body must become lower than atmospheric pressure. The main contributor to lowering the pressure is the contraction of the diaphragm, although the external intercostal muscles provide assistance by slightly expanding the rib cage (Figure 1. Muscles of Relaxed Inhalation. The lungs then expand, filling with air until the pressure is equal to atmospheric pressure. Next, the diaphragm relaxes and creates a smaller volume and higher pressure causing the air to leave the lungs. Forced or deep breathing enlists the help of additional muscles such as the sternocleidomastoid and the levatores costarum muscles to expand the rib cage to a greater extent and thus increase the pressure difference.

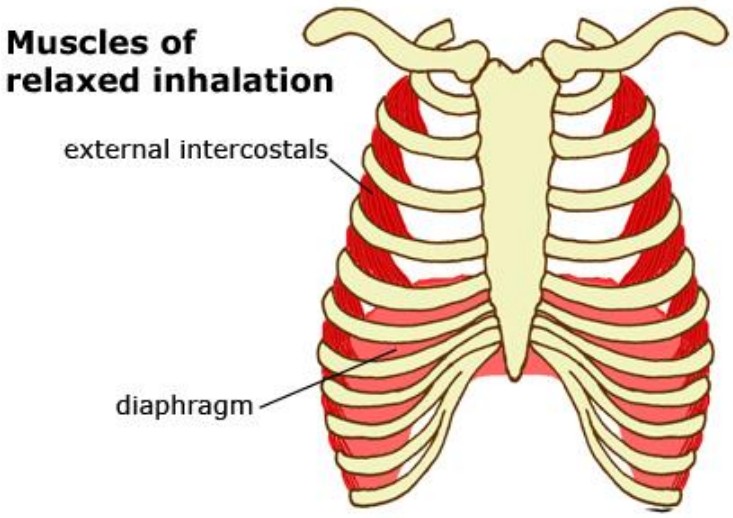

Figure 1. Muscles of Relaxed Inhalation [7]

The thorax consists of the thoracic vertebral column, 12 pairs of ribs, and the sternum. The thoracic vertebral column is composed of 12 individual vertebrae and is located posteriorly. From these vertebrae, 7 bilateral pairs of true ribs protrude anteriorly, connecting with the sternum via costal cartilage to provide reinforcement. Along with the true ribs, there are 3 pairs of false ribs that also connect to the sternum. However, these false ribs do not have individual pieces of costal cartilage for attaching to the sternum, but rather the ribs use the costal cartilage from the superior ribs. Finally, the last 2 pairs of ribs are called floating ribs as they protrude from the thoracic vertebral column, but do not bond to the sternum. The individual ribs are described as having two sides: cutaneous and pleural, where the cutaneous side has the larger curve length (Figure

2). For the purpose of this study, the strain along the rib was analyzed at 3 locations: 30%, 60% and 90% of the rib from posterior to anterior (Figure 2). By measuring strain at 3 different locations, the change in strain along the length of the rib can be determined. Additionally, the 30% and 60% locations are consistent with rib strain measurement in previous research [8].

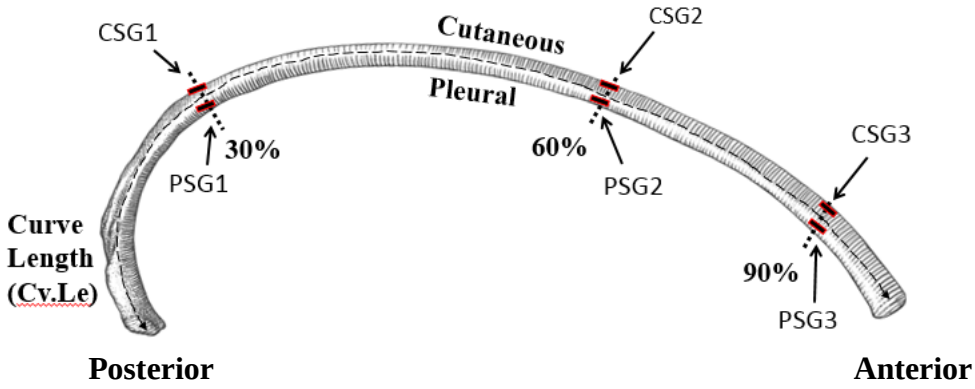

Figure 2. Labeled Rib

The objective of this project was to use a PMHS to determine the strain modes and magnitudes experienced by the ribs during ventilation. The hypotheses of the research include: 1) the ribs experience a straightening effect during ventilation producing compression on the cutaneous cortex and tension on the pleural cortex. 2) The greatest strain will be on the sternal side of the rib and will decrease along its length towards the vertebral side. However, to conduct this research project the PMHS system had to be validated. Therefore, one study was run to verify that the chestband strain gage

data from an in vivo system matched the PMHS system. A second study was also run to validate an open system PMHS model by comparing the cutaneous strain gage data from the closed PMHS system validated during study one.

Overall, the movement of the rib cage during ventilation is thought to produce a straightening effect on the individual ribs. This straightening effect appears reasonable when analyzing the movement of the rib cage during inspiration. As the rib cage rises and expands, the intercostal muscles could potentially be forcing the ribs to straighten slightly to achieve this motion. Additionally, the hypothesis that the sternal side exhibits an increased strain appears reasonable based on the ribs' connections to the rest of the skeletal system. The ribs connect anteriorly to the sternum by way of costal cartilage, while in the posterior the ribs directly articulate with the vertebral column. It is assumed that the costal cartilage is a point of weakness and will cause the sternal side of the ribs to experience more movement, and thus more strain, in comparison to the vertebral side.

Methods

This chapter will be divided into multiple sections: Subject Information, Phase I, Instrumentation for Phase II, PMHS Test: Phase II, Verification of Phase II, Evisceration Procedure, Instrumentation for Phase III, PMHS Test: Phase III, Verification of Phase III, and Data Analysis.

Subject Information

A male, fresh - frozen PMHS weighing 83 kg and having a height of 173 cm was used to conduct this test. The lungs and thorax had no issues as the cause of death was prostate cancer. Before testing began, a Bone Mineral Density (BMD) scan and a Computerized Tomography (CT) scan were performed on the PMHS. The subject had minimal scarring on the thorax and was confirmed non-osteoporotic via the BMD scan. The results showed the subject had normal BMD scores with a whole body T-Score of 0.4 and a Lumbar Spine T-Score of 1.9. Once the PMHS was confirmed as a viable subject, the PMHS was instrumented and prepared for testing.

Phase I

Phase I entailed collecting data of thorax movement during ventilation in vivo. Previous research had data measuring the change in curvature of the thorax during ventilation for live subjects that could be used to validate the PMHS model [9]. The previous research had measured the change in curvature and change in strain magnitude during normal and deep breaths in vivo using a chestband composed of strain gages. Data from 6 gages were available for use in this project to validate the PMHS system by comparing the change in curvature at the site of the strain gages from the in vivo subject to the PMHS.

Instrumentation for Phase II

The cutaneous side of the rib cage and the sternum were instrumented with a total of 44 general purpose strain gauges (VISHAY Measurement Group, CEA-06-062UW-350, Raleigh, NC). To access the ribs, the PMHS was placed in supine position and an

incision was made along the lateral aspect of the thorax from the shoulder to the bottom of rib 9. The skin and tissue was separated from the rib cage and reflected medially. The ribs were then carefully scraped with a scalpel and cleaned with ether to prepare the rib for strain gage installation. A drop of Loctite Super Glue Gel was then placed on each strain gage, as well as on the rib, and the strain gauge was gently pushed into place (Figure 3. Strain Gage Installation).

Figure 3. Strain Gage Installation

Once the glue was dried a voltmeter was used to verify the strain gauge was functioning correctly, then 2 coats of acrylic paint was applied to the strain gauge. After the paint had dried, a voltmeter was used a second time to verify the strain gauges did not have liquid trapped between them and the paint, but rather were in working order. These steps were repeated for each strain gage, and a more detailed list of the installation process can be found in Appendix A (Figure 4).

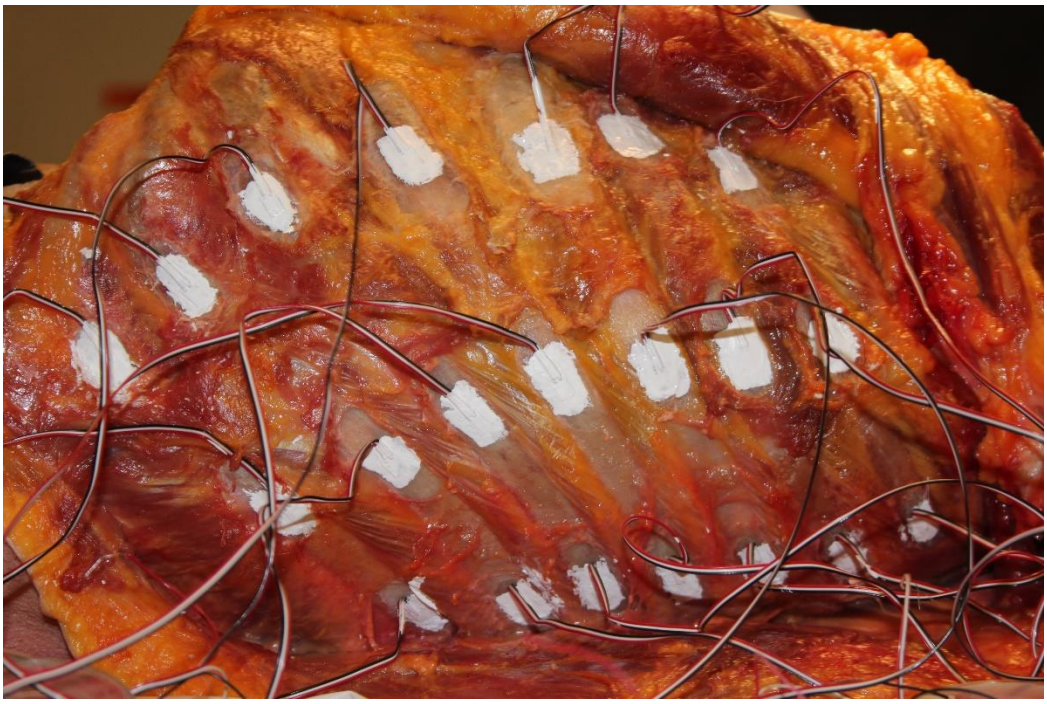

Figure 4. Strain Gauges on Left Side of Thorax

The strain gauges were installed on bilateral ribs 3-9 at 3 positions: posterior, lateral, and anterior on the cutaneous cortex (Figure 5). The use of 42 strain gages on the cutaneous cortex was justified by the need to determine any changes in strain mode on the surface of the rib.

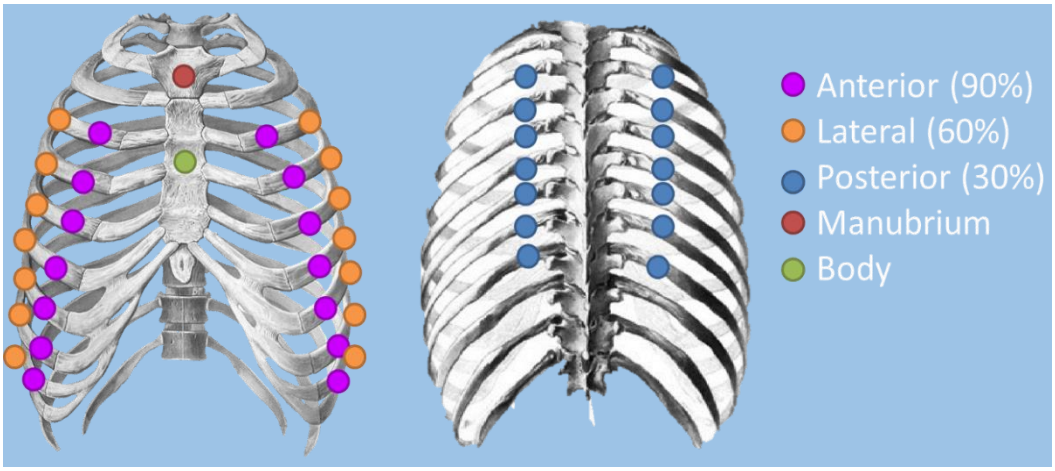

Figure 5. Strain Gauge Placement on Thorax

To determine changes in magnitude along the length of the rib and be consistent with previous research, the straight lengths and curve lengths of each rib were measured and the strain gages were then placed in the calculated 30%, 60%, and 90% of the rib positions [8]. Along with the ribs, the sternum was also instrumented with 2 strain gages to measure any strain that occurs in the sternum

To measure the movement of the thorax during ventilation, a chestband was used. A chestband is a collection of strain gauges spaced one inch apart that can be wrapped around the thorax, level with the center of the sternum (Figure 6), and used to measure the change in curvature of the thorax during ventilation.

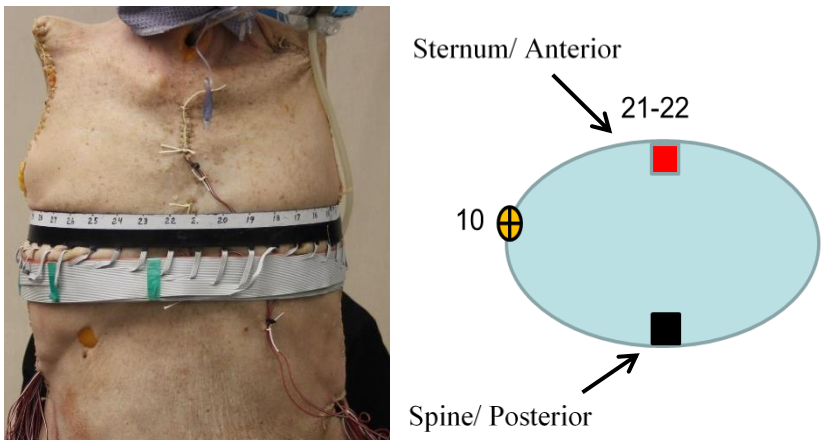

Figure 6. Chestband on Subject and Chestband Orientation

The chestband measured the orientation of the thorax at 40 different positions over time and the change in curvature of the thorax during PMHS testing could be compared with live subject testing to validate the authenticity of the in vitro test. The

chestband was wrapped around the PMHS in a clock-wise fashion with strain gages 21 and 22 on each side of the sternum (**Error! Reference source not found.**6).

PMHS Test: Phase II

Phase II consisted of a closed PMHS system where the thoracic organs were intact and the pleural cavity was sealed. The PMHS was placed in a seated, upright position using a bench and a head strap. Additionally, straps were wrapped around the knees to keep the hips of the PMHS in line with the shoulders (Figure 7).

Figure 7. Phase II PMHS Set-up

A resuscitation air bag connected to a tracheal tube was used to inflate the lungs of the PMHS. Average intrapulmonary pressure in vivo is around 14.7 psi, but due to rigor mortis and the PMHS inability to activate the intercostal muscles this pressure is not an accurate representation of the loading environment the ribs experience during

ventilation [10]. Instead, the intrapulmonary pressure was increased until the PMHS chestband data matched the live subject data. This pressure was then used for the remainder of the tests.

During Phase II, four tests were run with the chestband on the PMHS and two tests were run without the chestband. During all six tests the cutaneous strain gages collected data as a pattern of two normal breaths, two deep breaths, and then two normal breaths was conducted for each test (Table 1. Breathing Test Matrix Each test had a duration of 120 seconds and a sampling frequency of 1000 hz.

Table 1. Breathing Test Matrix Phase II

TEST MATRIX		
Test #	Breath Pattern (repeated for 120 s)	Phase: Instrumentation
Test 1-4	Normal (x2) Deep (x2) Normal (x2)	Phase II: Chestband & Cutaneous Strain Gages
Test 5-6	Normal (x2) Deep (x2) Normal (x2)	Phase II: Cutaneous Strain Gages Only

Verification of Phase II

The PMHS test was connected to an in vivo study in order to corroborate the accuracy of the data. A previous research project had live subjects wear a chestband composed of strain gages to measure the strain of the thorax during their natural and forced ventilation [9]. By having the PMHS wear a chestband during the first four trials,

the data from the change in curvature could be matched to the data from the live subjects, proving the validity of the PMHS set up.

Data from 6 strain gages located in the chestband: 16, 17, 21, 22, 26, and 27, were available from the previous study. The relationship shown in Equation 1, where ΔmV is the change in strain magnitude, $\Delta Curv$ is the change in curvature, and m is the slope, was used to corroborate the strain gage data from in vivo testing to the PMHS study.

Equation 1. Change in Curvature

$$\Delta Curv = m * \Delta mV$$

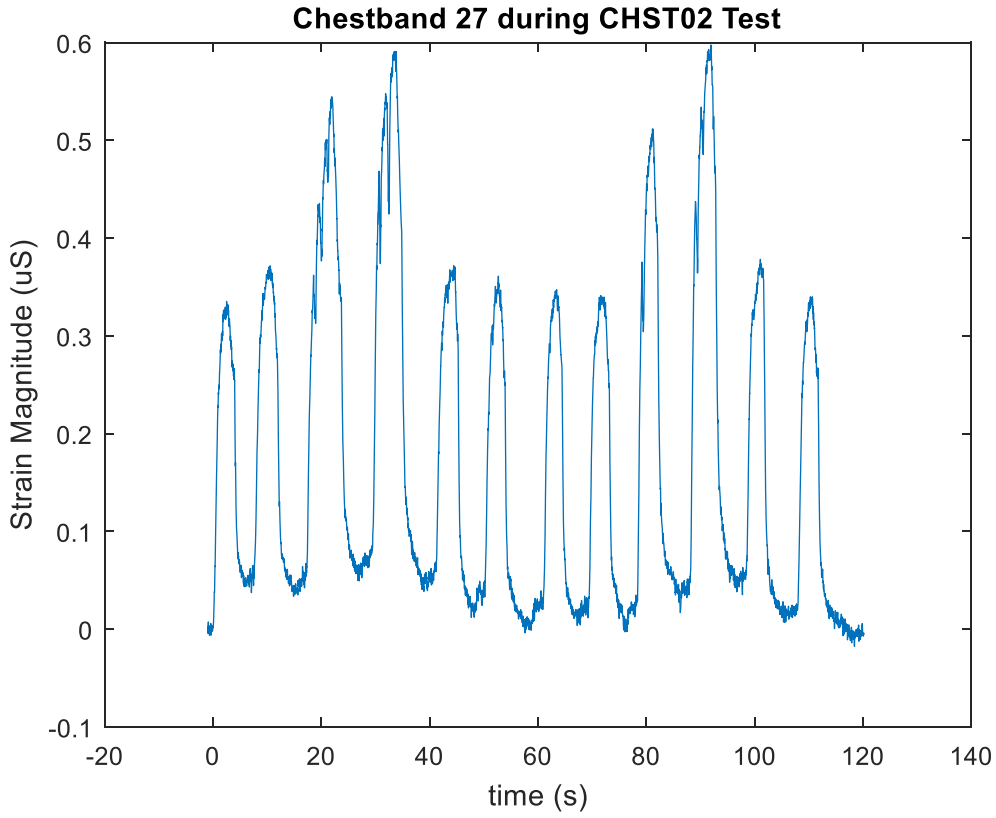

Figure 8. Chestband Strain Gage Plot

The slope for each strain gage was already calculated during in vivo testing and was used along with a value for ΔmV to calculate $\Delta Curv$ for the PMHS testing. The value for ΔmV was calculated by plotting strain vs. time for the chestband strain gages and measuring the difference from the minimum to the maximum point during a normal and a deep breath (Figure 8). The change in strain was measured for multiple breaths and the value was averaged before being used to calculate the change in curvature. The in vivo and PMHS change in curvature values were then compared using an unpaired t-test, where $\alpha = 0.05$, to validate the PMHS model by determining if the values had statistically significant differences.

Evisceration Procedure

A detailed, step-by-step procedure of the evisceration of the thoracic organs can be found in Appendix B. The following is a general description of the process.

The PMHS was placed in supine position and the neck of the PMHS was removed. A transverse cut of the skin was made above the sternal notch, then a midline incision was made 3-4" superiorly. All the muscles, arteries, veins, and nerves in the anterior portion of the neck, as well as the trachea and esophagus were then cut through. Finally, to completely severe the neck, a cut was made above the disc between C7 and T1 vertebrae.

After removing the neck, an incision was made horizontally over the abdomen. The abdominal wall was separated from the rib cage and reflected inferiorly. The ligaments attaching to the abdominal wall were severed and the greater omentum was pulled

superiorly to gain access to the intestines. The colon was detached and connecting arteries were severed. The esophagus was also tied off and cut inferiorly to the diaphragm. The stomach, duodenum, and pancreas were then detached, and the liver was removed by severing the falciform ligament and left triangular ligament. The kidneys and connecting urinary system was left intact.

To eviscerate the thoracic organs, the diaphragm was cut from the inferior margins of the ribs. The trachea, esophagus, and connecting organs were then pulled inferiorly and any attachments were severed.

Instrumentation for Phase III

After evisceration, the pleural side of the ribs was more accessible, however instrumenting strain gages was still a challenge. Therefore, the majority of the strain gages were installed on the lateral position at 60% of the rib. Specifically, the left and right sides of ribs 5-8 at the 60% mark had gages, with an additional gage at the 60% mark of left rib 4. Left and right ribs 6 and 7 were also instrumented with gages at the 30% and 90% positions. Lastly, right rib 5 had an additional gage at the 90% positon. The installation procedure for the gages was the same as the steps for the cutaneous gages. First the length of the curvature of the rib was measured using string and the location for the strain gage was marked (Figure 9). Next the location on the rib was cleaned and the strain gage was attached with glue. In total, the pleural side of the rib cage was instrumented with 18 strain gages. (Figure 10).

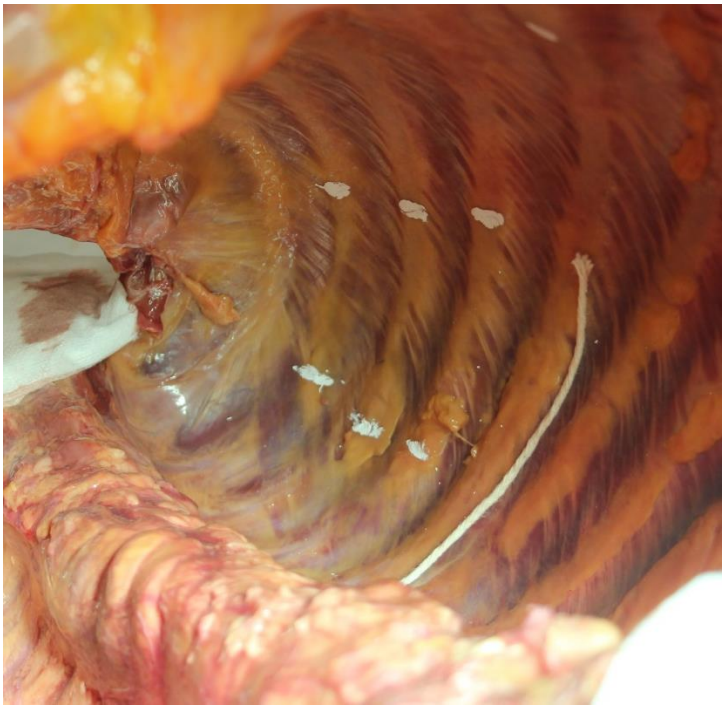

Figure 9. Measuring Length of Curvature of Rib on Pleural Cortex

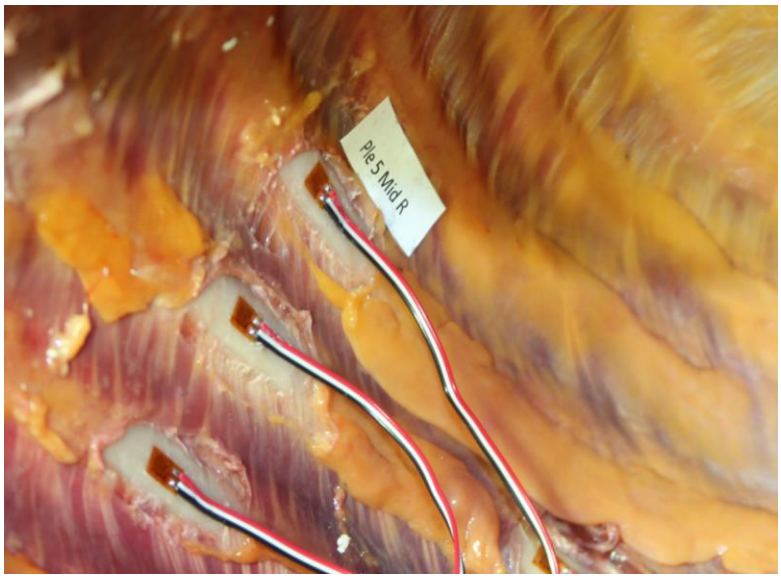

Figure 10. Strain Gage Installation on Pleural Cortex on Right Side of Rib Cage

Just as with the cutaneous rib gages, the use of 18 strain gages was warranted to quantify any changes in strain mode on the rib. The pleural side of the ribs is more difficult to access than the cutaneous side, but no significant changes could be made

without compromising the integrity of the thorax. Therefore strain gages were placed in the 30%, 60%, and 90% of the rib positions to the best of the researchers' ability. The same installation procedure as for the cutaneous side of the rib was followed.

To replicate the process of ventilation, an air bladder was inserted into the thoracic cavity and inflated using a resuscitation pump (Figure 11). To install the air bladder, it was first connected to tubing and the cadaver was placed in supine position. Next, the tubing was fed through the opening to the thorax and emerged from the superior opening to the thoracic cavity. The air bladder was then placed in the thorax and zip ties were used to secure the tubing and air bladder to the fixture and prevent the bladder from sliding down during testing.

Figure 11. Air Bladder

Finally, a Hybrid III 50th percentile ATD abdomen was inserted into the abdomen and sutured closed to account for the removal of the abdominal organs (Figure 12).

Figure 12. ATD Abdomen

PMHS Test: Phase III

Phase III was an open PMHS system, meaning the pleural cavity was open to air and the thoracic organs had been eviscerated to allow for instrumentation of the pleural cortex with strain gages. During Phase III, the PMHS was placed in a seated position on a bench and the thorax was held in an upright position by securing the spine to the fixture with zip ties (Figure 13).

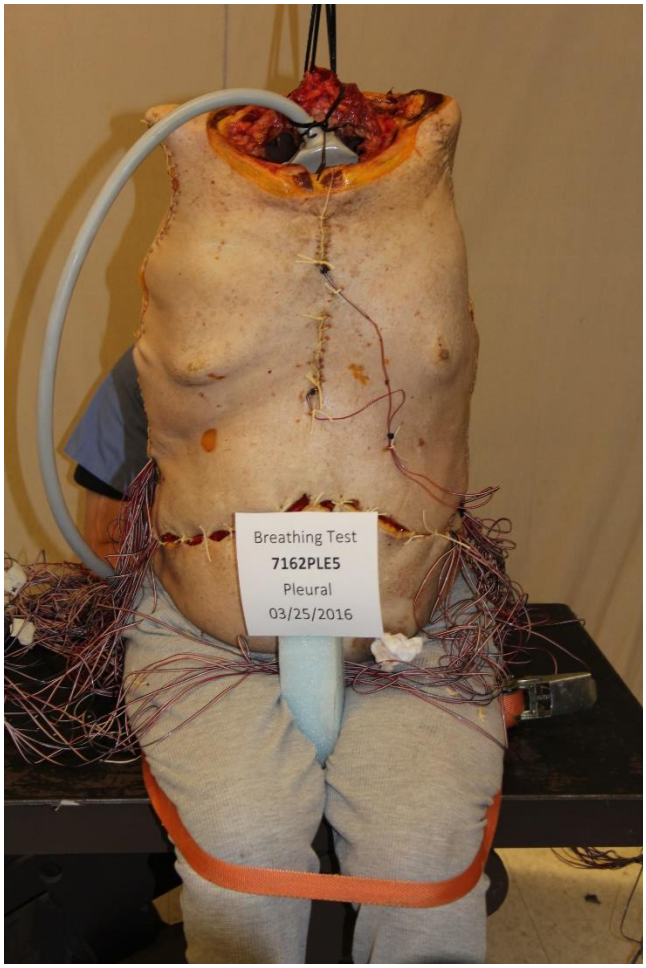

Figure 13. Open System Phase III PMHS Setup

During Phase III, six tests were run with cutaneous strain gages and pleural strain gages on the ribs. Because an air bladder was used instead of lungs, the pressure required to inflate the bladder in a way that produced rib movement consistent with Phase II was

unknown. Therefore, two trials of inhalation and exhalation were conducted with the pressure reaching a maximum of 120 cm H_2O instead of using the breath pattern (Table 2). By inflating the air bladder to such a high pressure, a curve of changing strain magnitude based on pressure is created. The appropriate pressure required to produce rib movement similar to the closed PMHS system in Phase II can then be determined by finding what pressure produces a strain magnitude that matches the strain magnitude in Phase II.

Table 2. Breathing Test Matrix Phase III

TEST MATRIX		
Test #	Breath Pattern	Phase: Instrumentation
Test 7-12	Inflate air bladder to maximum pressure of air pump (approx. 120 cm H_2O) then deflate (Total Duration 60 s) (x2)	Phase III: Cutaneous & Pleural Strain Gages

Verification of Phase III

The open system PMHS model used in Phase III was verified by comparing its cutaneous strain gage data to the closed PMHS system in Phase II. The average strain experienced during a normal and deep breath was measured during Phase II testing. These average values were then compared to the values in Phase III by plotting the cutaneous strain values to see if similar strains could be produced in an open system and conducting an unpaired t-test to see if there were statistically significant differences between the values.

Data Analysis

Data was collected using DTS Slice Pro data acquisition system (Diversified Technical System, Seal Beach, Ca) with a sampling frequency of 1000 hz and analyzed via MATLAB. To determine the strain mode on the cutaneous and pleural cortexes, all strain gage data was multiplied by -1 to account for the flipping of polarity that occurs during data collection. Next the tests for each strain gage were plotted and the graph was analyzed to discover the strain mode. If the plot was composed of negative values then the rib was experiencing compression at that location. However, if the values were positive then the rib was experiencing tension.

The change in strain magnitude along the length of the rib was determined by zeroing the data from each gage and then calculating the average maximum strain for a normal and deep breath at each gage location. The different strain magnitudes were then compared between rib positions.

Results: Validating PMHS System

In order to validate Phase II, the change in curvature was calculated for the 6 chestband gages from Phase I. When conducting the testing during Phase II, chestband gage 16 was lost, therefore 5 gages were used to compare between Phase I and II. To determine the change in strain magnitude during Phase II, each normal and deep breath was measured during a test. After averaging the change in strain during a normal breath and a deep breath, the change in curvature for Phase II was successfully calculated using equation 1 and compared with Phase I change in curvature values as seen in Table 3.

Table 3. Chestband Change in Curvature Calculations

		Normal Breath			Deep Breath		
Chestband Gage #	slope	Avg dmV (Phase II)	ΔCurv (Phase I)	ΔCurv (Phase II)	Avg dmV (Phase II)	ΔCurv (Phase I)	ΔCurv (Phase II)
17	0.000672	0.2888	0.0003	0.0002	0.765	0.0003	0.0005
21	0.000666	0.6688	0.0003	0.0004	1.0125	0.0003	0.0007
22	0.000682	0.0517	0.0003	0.0000	0.33	0.0003	0.0002
26	0.000626	0.2688	0.0003	0.0002	0.6350	0.0003	0.0004
27	0.000634	0.3256	0.0005	0.0002	0.5325	0.0005	0.0003

An unpaired t-test was then conducted to determine if the results were statistically different. Using $\alpha = 0.05$, the P-value for both normal and deep breaths, 0.1396 and 0.3406 respectively, had a value greater than 0.05, thus proving that there was no statistical difference between the in vivo test and PMHS test. Therefore, the closed system PMHS model was validated.

To determine if the open PMHS system in Phase III was able to match the cutaneous data from Phase II, maximum strain magnitude values in Phase II were compared to the closet equivalent value in Phase III. Because Phase III consisted of two repetitions of inflating to a pressure of 120 cm H_2O and then deflating, while Phase II consisted of a pattern of two normal breaths, two deep breaths, and two normal breaths repeated for 120 s, the plots could not be directly compared. Rather, the Phase III plots were examined to see if they had values equivalent to the maximum strain magnitude values in Phase II. An unpaired t-test was then conducted to determine if the values differed significantly. Using $\alpha = 0.05$, the P-value for the maximum cutaneous strain magnitude value during Phase II compared to the closest equivalent value in Phase III was greater than 0.05 for each rib location analyzed (Table 4). Consequently, there was

no statistical difference between the closed PMHS system and open PMHS system, thus validating the open system PMHS model.

Table 4. P-Values for Cutaneous Strain of Phases II & III T-Test

Normal Breath			
Left Rib #	Posterior P-Value	Lateral P-Value	Anterior P-Value
3	0.996	0.967	0.996
4	0.959	0.995	0.999
5	0.994	0.978	0.999
6	0.954	0.995	0.873
7	0.981	0.992	0.926
8	0.948	0.936	0.981
9	0.992	0.998	0.705
Right Rib #			
3	0.957	0.981	0.9999
4	0.961	0.999	0.999
5	0.374	0.993	
6	0.611	0.999	0.971
7	0.894	0.986	0.989
8	0.961	0.964	0.356
9	0.767	0.994	0.952

Deep Breath			
Left Rib #	Posterior P-Value	Lateral P-Value	Anterior P-Value
3	0.256	0.696	0.983
4	0.802	0.959	0.992
5	0.828	0.794	0.999
6	0.888	0.613	0.97
7	0.865	0.665	0.973
8	0.865	0.908	0.992
9	0.856	0.708	0.996
Right Rib #			
3	0.987	0.993	0.999
4	0.881	0.999	0.999
5	0.108	0.815	
6	0.000	0.786	0.921
7	0.895	0.926	0.993
8	0.219	0.995	0.979
9	0.229	0.915	0.968

Legend	
Broken	
T-test:	$\alpha = 0.05$
Significant	

It was determined that Phase III successfully imitated the cutaneous strain for the majority of the locations, with only the posterior positon of right rib 6 having a significant difference between Phase II and Phase III.

Results PMHS

Upon plotting the tests for each strain gage, it was determined that the lateral and anterior positions of the pleural cortex were in tension, while the posterior position was in compression. In contrast, the lateral and anterior positions of the cutaneous cortex was in compression, while the posterior position was in tension. For example, when comparing Figure 14. Cutaneous Rib 6 Anterior Position in Tension Figure 15. it can be noted that

the gage data on the cutaneous cortex in the anterior position have positive values and the rib is therefore in tension, while the gage data on the pleural cortex have negative values and the rib is therefore in compression. However, this pattern of strain mode is not consistent with all rib locations as seen in Table 5.

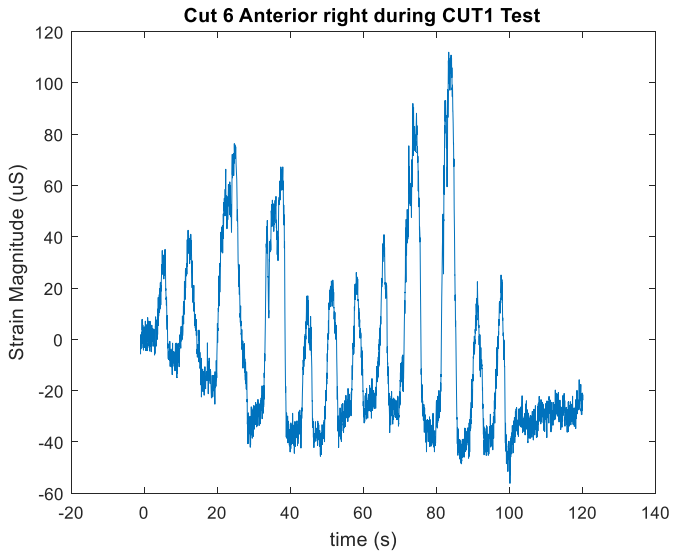

Figure 14. Cutaneous Rib 6 Anterior Position in Tension

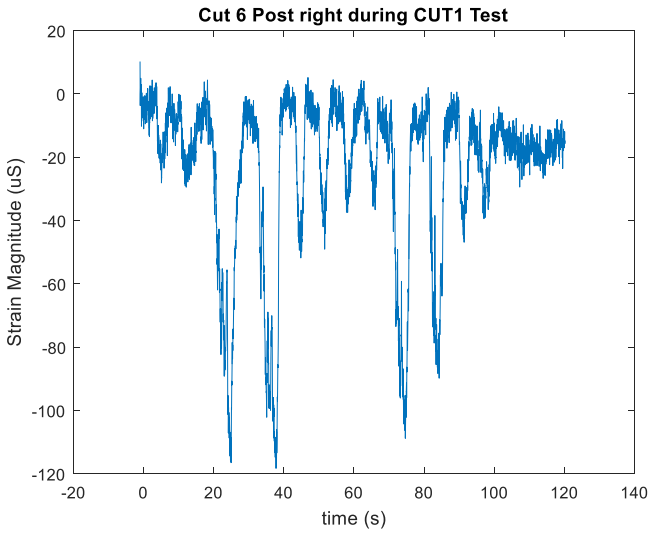

Figure 15. Cutaneous Rib 6 Posterior Position in Compression

Table 5. Strain Mode for each Strain Gage Location

Pleural Ribs					
Position	4	5	6	7	8
Posterior					
Lateral					
Anterior					

Legend	
compression	
tension	
transitioning	
broken	

Left Cutaneous Rib - Phase II							
Position	3	4	5	6	7	8	9
Posterior							
Lateral							
Anterior							

Right Cutaneous Ribs - Phase II							
Position	3	4	5	6	7	8	9
Posterior							
Lateral							
Anterior							

When comparing the strain magnitudes in the closed PMHS system in Phase II along the length of the rib, no pattern of strain magnitude based on position was noted. As seen in Table 6, the calculated average strain magnitude tends to be greater at the posterior and anterior positions than the lateral position. However, when comparing the anterior and posterior positions, one location does not appear to have a greater strain magnitude than the other.

Table 6. Average Strain Magnitudes on Cutaneous Cortex of Left Ribs

Cutaneous Cortex Strain Gage Position	Left Rib #	Avg Strain Magnitude for Normal Breath	Avg Strain Magnitude for Deep Breath
Posterior	3	-155	-277
Lateral		42	59
Anterior		234	409
Posterior	4	68	133
Lateral		-152	-260
Anterior		-395	-679
Posterior	5	121	252
Lateral		-59	-111
Anterior		-351	-691
Posterior	6	117	232
Lateral		99	199
Anterior		61	96
Posterior	7	149	307
Lateral		60	111
Anterior		32	45
Posterior	8	138	291
Lateral		83	147
Anterior		100	162
Posterior	9	63	120
Lateral		20	62
Anterior		36	88

As seen in Figures 16, 17, 18, and 19, the strain magnitude for Phase II varies from each position, but one location is not consistently significantly greater than any other location. Additionally, looking at Figures 20, 21, 22, and 23, the difference in strain magnitude along the length of the rib can also be seen by calculating the change in

magnitude between each location (Anterior to Posterior, Anterior to Lateral, and Lateral to Posterior)

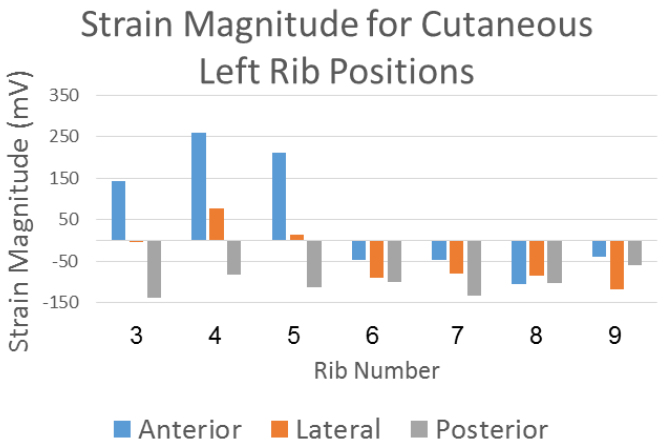

Figure 16. Left Cutaneous Strain

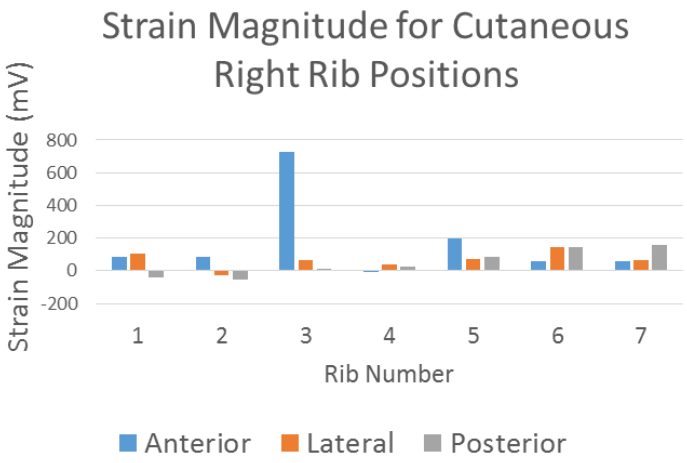

Figure 17. Right Cutaneous Strain

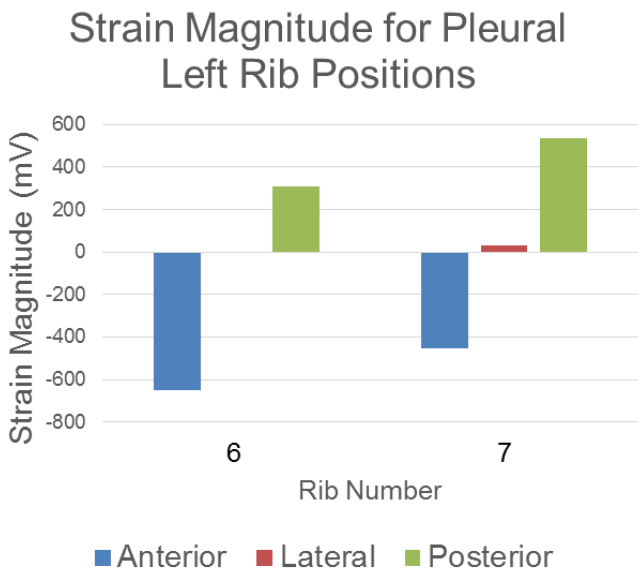

Figure 18. Left Pleural Strain

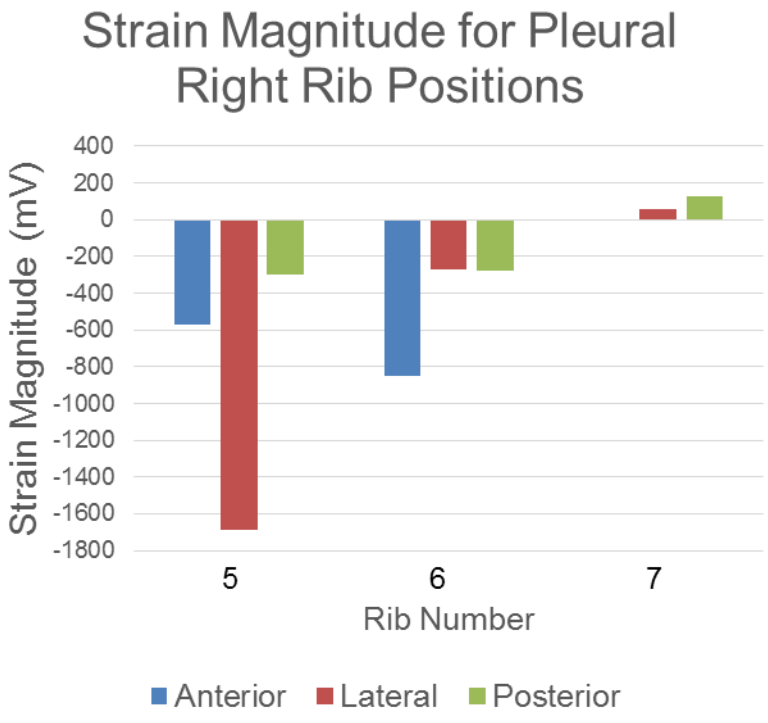

Figure 19. Right Pleural Strain

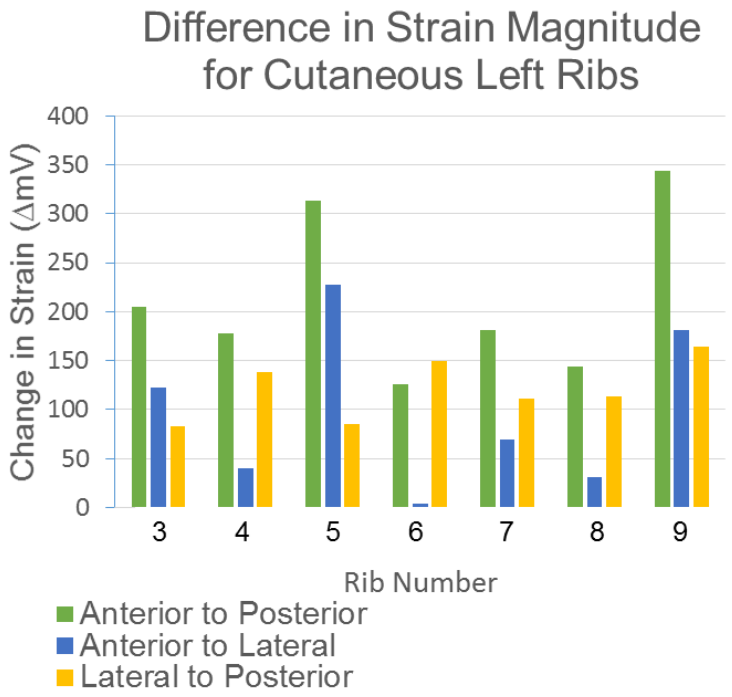

Figure 20. Left Change in Cutaneous Strain

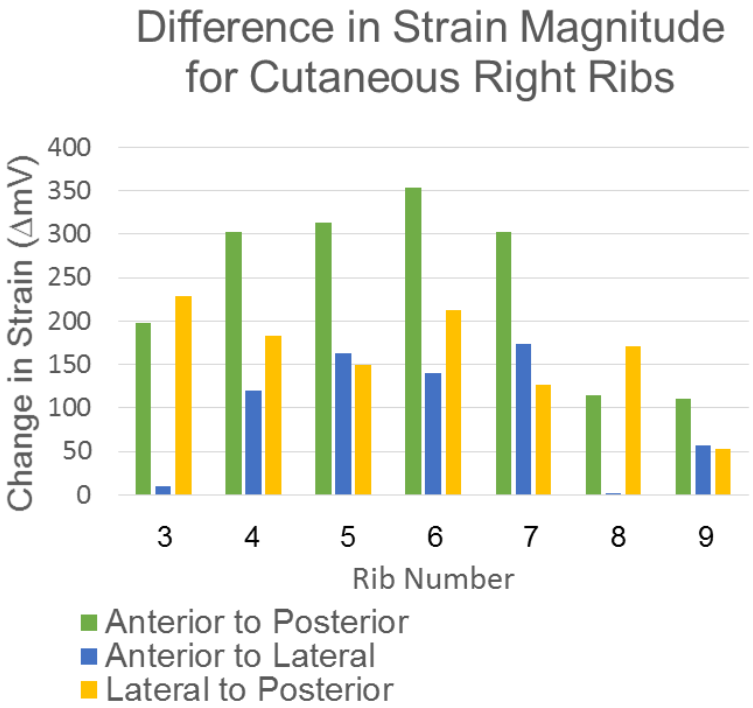

Figure 21. Right Change in Cutaneous Strain

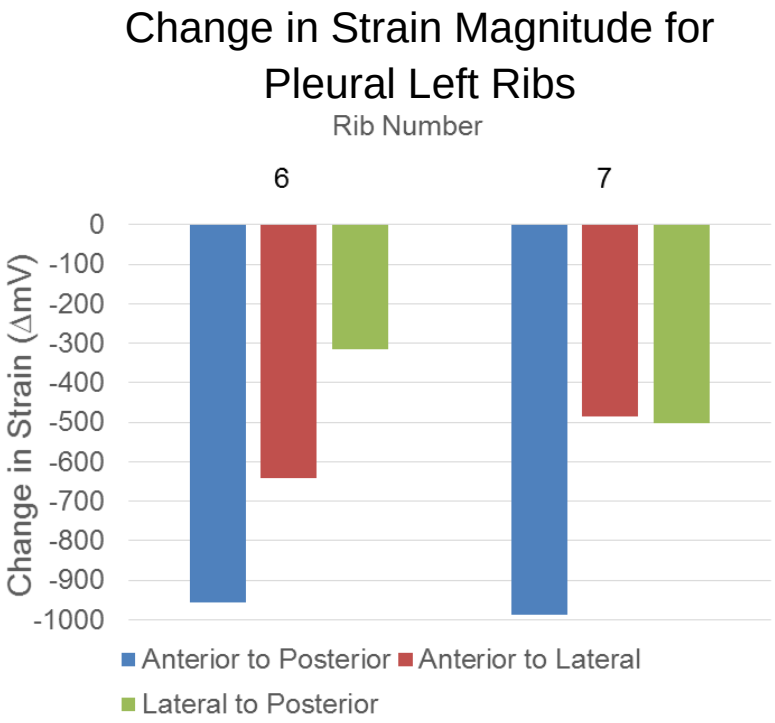

Figure 22. Left Change in Pleural Strain

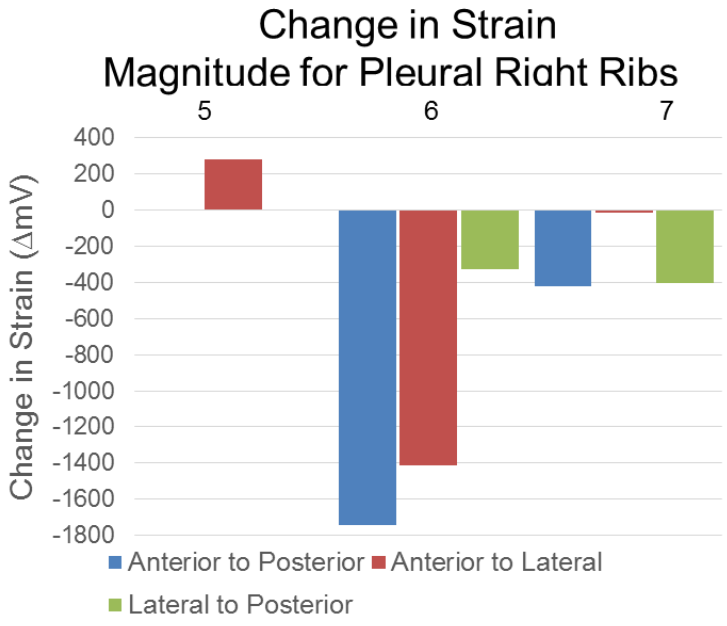

Figure 23. Right Change in Pleural Strain

Discussion

Before analysis of the hypotheses could be conducted, the closed and open PMHS models had to be validated. The closed PMHS system was successfully verified when comparing chestband data to in vivo studies. A t-test revealed no significant differences between the chestband gage values for change in curvature. Additionally, the open PMHS system was validated after comparing cutaneous strain gage data with the closed PMHS system where a t-test confirmed no statistically significant differences. These results show that it is possible to create a model to simulate the normal loading environment that ribs are adapted to during ventilation.

The hypotheses of the research were:

1) The ribs experience a straightening effect during ventilation producing compression on the cutaneous cortex and tension on the pleural cortex.

2) The greatest strain will be on the sternal side of the rib and will decrease along its length towards the vertebral side.

The first hypothesis was proven to be partially true. After analyzing the strain mode during Phase II and Phase III, it was noted that the cutaneous cortex was in compression on the lateral and anterior locations, consistent with the hypothesis. However, the posterior position was in tension on the cutaneous cortex. Similarly, the lateral and anterior positions of the pleural cortex were in tension, consistent with the hypothesis, while the posterior position was in compression. This pattern of strain mode likely results from the ribs experiencing a straightening effect as the lungs inflate.

The second hypothesis stating that the strain magnitude will be greatest at the anterior location on the rib and decrease posteriorly was proven to be false. Although the strain magnitude did change based on location, the strain magnitude did not vary systematically based on the position on the rib. This change in strain magnitude can be seen in figures 20, 21, 22, and 23, and more statistical tests will need to be run to see if the change in strain magnitude between any of the locations is significant.

Limitations and Improvements

During instrumentation for Phase II, the pleural cavity was perforated on the right side of the thorax. The tear was sealed with dental dam and skin adhesives, but this perforation may have influenced the results of this study (Figure 24). However, because the chestband values between Phase I and Phase II matched, the perforation of the pleural cavity most likely had no effect. Additionally, this perforation did not affect Phase III as the PMHS model was already an open system during this phase.

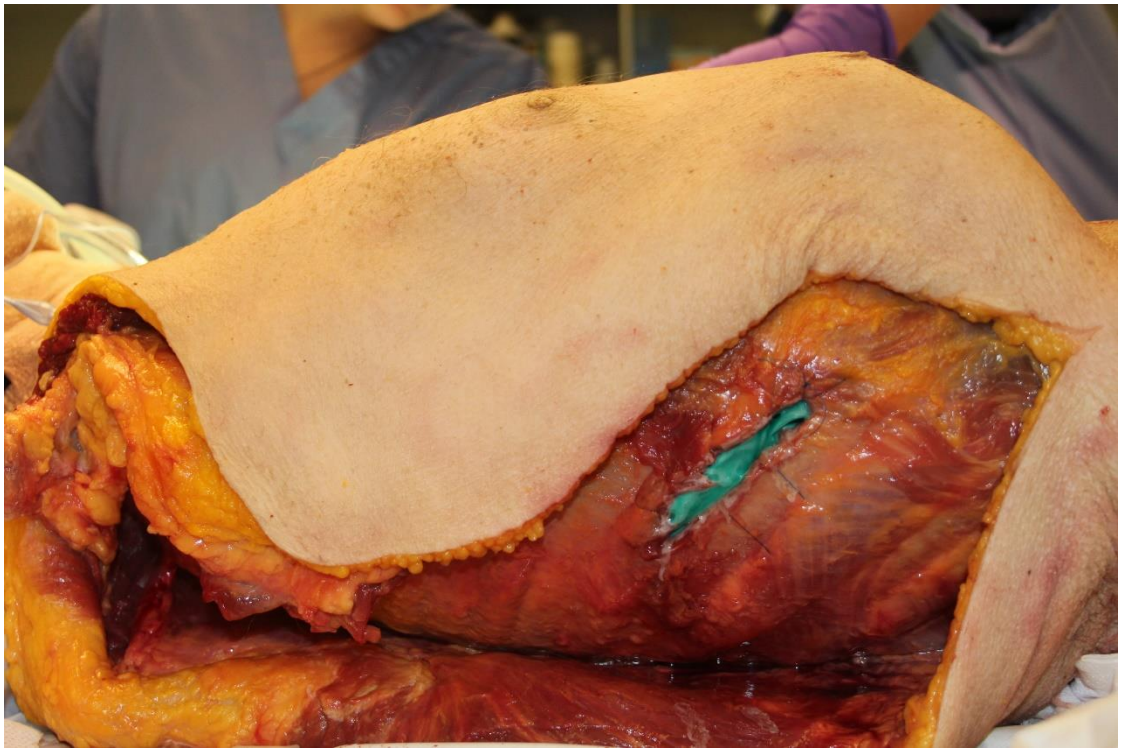

Figure 24. Seal for Perforation of Pleural Cavity

This study could be improved by increasing the number of strain gages on the pleural cortex of the ribs. The majority of the pleural gages were on the lateral position of the rib for this study, but by increasing the number of gages on the posterior and anterior positions, the strain magnitude along the length of the pleural cortex could be studied. Additionally, two air bladders could be used in Phase III instead of one in order to more closely mimic human lungs.

Conclusion

This research project discovered that it is possible to model the regular loading environment that ribs are adapted to. Both a closed PMHS system and an open PMHS

system were validated as models for the rib loading environment. Moreover, it has been determined that the strain magnitude varies with position on the rib, although no discernible pattern is evident. The strain mode has also been determined to vary based on the cortex of the rib.

References

[1] Kindig, M., Lau, A.G. & Kent, R.W., 2011. Biomechanical Response of Ribs Under Quasistatic Frontal Loading. *Traffic Injury Prevention*, 12(4), pp.377–387.

[2] Stitzel, J.D. et al., 2003. Defining Regional Variation in the Material Properties of Human Rib Cortical Bone and Its Effect on Fracture Prediction. *Stapp Car Crash Journal*, 47(October), pp.243–265.

[3] Fazzalari, Nicola L. "Trabecular Microfracture." *Calcified Tissue Internatioanl* 53 (1993): S143-S147. Print.

[4] Ebacher, V., Tang, C., McKay, H., Oxland, T. R., Guy, P., & Wang, R. (2007). Strain reidstriubtion and crakcing behavior of human bone during bending. *Bone*, *40*, 1265-1275.

[5] Burr, D. (2003). Microdamage and bone strength. *Osteoporos Int*, *14*, S67-S72.

[6] McCool, F. D., Loring, S. H., & Mead, J. (1985). Rib cage distortion during voluntary and involuntary breathing acts. Journal of Applied Physiology, 58(5).

[7] The muscles of human respiration. (n.d.). Retrieved from Comparative Anatomy website: http://inside.ucumberlands.edu/academics/biology/faculty/kuss/courses/Respiratory%20system/Muscles%20of%20Human%20Resp.htm

[8] Schafman, M., Kang, Y.-S., Moorhouse, K., & Agnew, A. M. (n.d.). The effect of age on the structural properties of ribs in dynamic frontal loading. *2014 Ohio State University Injury Biomechanics Symposium*.

[9] Cagle, D. (2011). Investigation of respiration induced strain caused on the rib (Unpublished undergraduate's thesis). The Ohio State University, Columbus, OH/USA.

[10] Marieb, E. (n.d.). The respiratory system: Mechanics of breathing. In E. Marieb (Author), *Human anatomy & physiology* (4th ed., pp. 813-820).

Appendix A

Strain Gauge Installation:

___ Expose right ribs three through nine with lateral incision and folding over of skin
___ Take measurements of the rib curvature length
___ Clean site of strain gage on right ribs three through nine by scraping with scalpel, and drying with ether where the strain gauges will be placed
___ Apply gel glue to spot on bone and to strain gauge and lead wires, then press together using dental dam for ~ 3 minutes until dry
___ Test strain gauge: Red & black (350 Ω), red & white (350Ω), white & black (0 Ω)
___ Strain relief the gauge wires near the rib using suture
___ Bundle all gauge wires and strain relief to skin
___ Take picture and record location of strain gauges
___ Expose left ribs three through nine
___ Repeat tissue measurement and strain gauge placement for left thorax
___ Take picture and record location of strain gauges
___ Clean and dry sternal strain gauge location by scraping and ether
___ Repeat tissue measurement, strain gauge placement, and data recording for sternum
___ Check that all strain gauges are working using voltmeter
___ Strain relief the gauge wires near the rib using suture
___ Bundle all gauge wires and strain relief to skin
___ Suture incision closed

Appendix B

Thoracic Organ Evisceration Procedure

Eviscerate Abdominal Organs

1) Place cadaver in supine position with a block placed transversely under the lumbar region
2) Make skin incisions as shown in Figure 1 and reflect skin flaps laterally. Also remove Camper's and Scarper's fascia

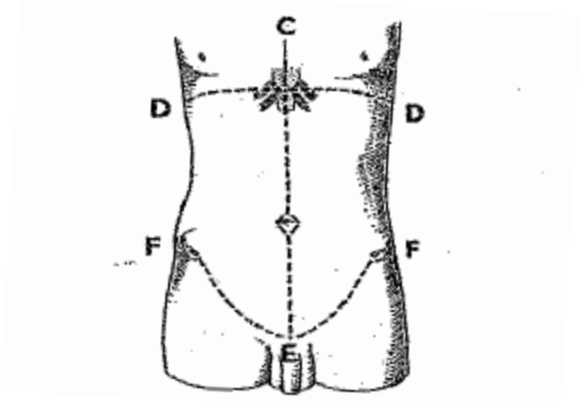

Figure 1: Abdominal skin incisions

3) Make a 3 cm vertical incision just inferior to the xyphoid process, cutting through Rectus abdominis muscle
4) Pull the abdominal wall anteriorly, to create a gap between the wall and the abdominal contents, and extend the vertical incision to the pubic symphysis, making sure to cut around the umbilicus
5) Place one hand inside the left abdominal cavity to separate its contents from the abdominal wall and with the other hand detach the abdominal wall from the rib cage
6) Start at the xyphoid process and follow the inferior border of the rib cage and carry the cut to the left iliac crest, the reflect the abdominal wall inferiorly
7) Detach the falciform ligament near the abdominal wall and sever the ligamentum teres, then reflect the right abdominal wall in the same manner as the left
8) Stretch the greater omentum cranially to reveal the intestines
    - Omentum, rectum, duodenum, jejunum, ileum, and colon
9) Tie two strings 2.5 cm apart tightly around the rectum and cut the rectum between the strings
10) Cut the inferior mesenteric artery close to the abdominal aorta
11) Cut through the mesentery of the sigmoid colon

12) With the fingers detach the descending colon from the posterior abdominal wall and cut through the phrenicocolic ligament
13) Detach the ascending colon from the posterior abdominal wall
14) Pull the transverse colon with the attached greater omentum caudally, and sever the origin of the superior mesenteric artery
15) Sever the celiac trunk at its origin from the aorta
16) Tie a string around the esophagus close to the diaphragm and cut just inferior to the diaphragm
17) Free the stomach completely so that it is only attached to the duodenum and blood vessels, and cut the vagal branches to the celiac plexus of nerves
18) Sever the suspensory ligament of the duodenum close to the duodenojejunal junction
19) With fingers, detach the duodenum and pancreas from the posterior abdominal wall
20) Lift the liver anteriorly and superiorly then cut through the inferior vena cava close to the dorsal surface of the liver
21) Cut the falciform ligament between the diaphragm and the diaphragmatic surface of the liver
22) Cut the left triangular ligament and the anterior portion of the coronary ligament
23) Pull the liver inferiorly then cut the IVC near the diaphragm
24) Cut the remaining portion of the coronary ligament and the hepatorenal ligament
25) Remove the detached GI tract with the liver, pancreas, and spleen
26) Remove the parietal peritoneum
27) Remove the kidneys from the renal fascia and fatty capsule
28) Dissect the kidneys out and remove the fatty renal capsule and renal fascia from the posterior abdominal wall

Remove Pelvis and Lower Limbs

1) Keep subject in supine position with a block placed transversely under the lumbar region
2) Use reciprocating saw to cut through the spine below the 12^{th} thoracic vertebrae

Remove Head and Neck

1) Keep subject in supine position
2) Open neck and cut through neck muscles
    - Make a skin transverse cut of skin above sternal notch
    - Make a midline incision 3-4" superior
    - Reflect skin superior lateral on both sides.
    - Cut through all muscles in the anterior portion of the neck
    - Cut trachea and esophagus
    - Cut jugular vein and carotid artery & brachial plexus of nerves
    - Cut above disc between C7 and T1 vertebrae

Eviscerate Thoracic Organs

1) Clean off inferior edge of ribs 10, 11, 12 to define the edge of the cage
2) Remove diaphragm from inferior margins of ribs
3) Place arm up through inferior outlet of thoracic cage
4) Grab trachea, esophagus, etc. and pull inferiorly
5) As you pull inferiorly, remove adhesions between thoracic cage and lungs
    - Lungs, heart, etc will pull up and off of vertebral column.
    - Pull "block" out of cage inferiorly